Confocal imaging of protein distributions in porous silicon optical structures

2007 J. Phys.: Condens. Matter 19 395009

(http://iopscience.iop.org/0953-8984/19/39/395009)

IOP PUBLISHING JOURNAL OF PHYSICS: CONDENSED MATTER

J. Phys.: Condens. Matter **19** (2007) 395009 (7pp) doi:10.1088/0953-8984/19/39/395009

Confocal imaging of protein distributions in porous silicon optical structures

Luca De Stefano[1,3] **and Sabato D'Auria**[2]

[1] Institute for Microelectronics and Microsystems, Department of Naples, National Council of Research, Via P Castellino 111, 80131 Naples, Italy
[2] Institute of Protein Biochemistry, National Council of Research, Via P Castellino 111, 80131 Naples, Italy

E-mail: luca.destefano@na.imm.cnr.it

Received 13 February 2007, in final form 7 March 2007
Published 30 August 2007
Online at stacks.iop.org/JPhysCM/19/395009

Abstract

The performances of porous silicon optical biosensors depend strongly on the arrangement of the biological probes into their sponge-like structures: it is well known that in this case the sensing species do not fill the pores but instead cover their internal surface. In this paper, the direct imaging of labelled proteins into different porous silicon structures by using a confocal laser microscope is reported. The distribution of the biological matter in the nanostructured material follows a Gaussian behaviour which is typical of the diffusion process in the porous media but with substantial differences between a porous silicon monolayer and a multilayer such as a Bragg mirror. Even if semi-quantitative, the results can be very useful in the design of the porous silicon based biosensing devices.

(Some figures in this article are in colour only in the electronic version)

1. Introduction

Porous silicon (PSi) is a very versatile tool for biosensing investigators due to its intrinsic properties but also to the simplicity of the fabrication process. PSi is obtained by electrochemical dissolution of doped crystalline silicon in hydrofluoridic acid–ethanol based solution: by changing the characteristic of the wafer and the values of the process parameters, many morphologies (from the chaotic sponge-like to the ordered pillars geometries) can be produced [1]. The tuning of the specific area and of the pore sizes can be used to optimize the PSi–biomolecule interaction. Another key feature of PSi is the high optical quality that PSi multilayers exhibit: many label-free optical devices have been proposed and demonstrated in biochemical sensing experiments, ranging from the simple monolayer [2, 3], which optically

[3] Author to whom any correspondence should be addressed.

acts as a Fabry–Perot interferometer, to the more complicated Bragg mirrors [4], optical microcavities [5], rugate filters [6] and Thue–Morse sequences [7], which all show resonant characteristic wavelengths. These PSi optical sensors are based on the changes of the reflectivity due to the exposure to the target analytes which penetrate into the pores and replace the air there. The consequence is an increase of the average refractive index of the PSi structure. The selectivity, i.e. the ability to identify a target analyte in a heterogeneous mixture, is assured by the affinity of the biomolecular probe with the analyte. The sensitivity of this kind of device can be defined as the ratio between the change of the wavelength shift and the change in the average refractive index of the structure. In biosensing affinity experiments, the change in the average refractive index is not really due to the filling of the pores since the biomolecular probes only cover the internal surface of the pores: a major role is played by the volume–surface ratio and by the distribution of the biomolecules over and in the inner space of the porous bulk. Some recent studies have been focused on the optimization and the sensitivity analysis of these devices [8–10]. Even if these models are quantitative, they assume a uniform distribution of active sites, where the ligand-binding events could take place, inside the whole available volume of the PSi. This assumption is quite approximate since any biological solution cannot uniformly penetrate everywhere in the porous matrix: the presence of the air in the smallest pores and the liquid–surface interaction prevents the filling of each empty pore and hence the possibility of distributing the probes in the PSi bulk equally. In this work, we have used laser scanning confocal microscopy to directly image the distribution of labelled proteins infiltrated and covalently linked to the PSi surface.

2. Materials and methods

The technique of laser scanning confocal fluorescence microscopy has become an essential tool in biology and the biomedical sciences, since it has the ability to control depth of field, eliminate the background information away from the focal plane and, thus, the capability to collect serial optical sections from thick specimens. In a conventional wide field optical fluorescence microscope, secondary fluorescence emitted by the specimen often occurs through the excited volume and obscures the resolution of features that lie in the objective focal plane. Confocal microscopy is able to exclude secondary fluorescence in areas removed from the focal plane from resulting images. The principle of laser scanning microscopy is diagrammatically presented in figure 1: the light emitted by the laser system is reflected by a dichromatic mirror and scanned across the specimen in a defined focal plane, so that the fluorescence emitted from points on the specimen pass back through the dichromatic mirror and are focused as a confocal point at the detector pinhole aperture.

The fluorescence emission that occurs at points above and below the objective focal plane is not detected by the photomultiplier and does not contribute to the resulting image. Refocusing the objective in a confocal microscope shifts the excitation and emission points on a specimen to a new plane that becomes confocal with the pinhole apertures of the light source and detector [11]. Confocal imaging of PSi photoluminescence has been successfully used to characterize the PSi emission properties and obtain three-dimensional (3D) profiles of porous silicon structures reconstructed from confocal slices [12, 13]. Our measurements were performed on a laser scanning microscope system Leica SP2 AOBS, having an axial minimum resolution of about 0.15 μm. The porous silicon layer was obtained by etching a highly doped p^+-silicon ($\langle 100 \rangle$ oriented, 0.05 Ω cm resistivity) in an HF–ethanol solution (48%, 1:1) at room temperature with a current density of 145 mA cm^{-2} for 46 s. The layer thickness was about 12 μm and the porosity about 70% (values estimated by fitting the optical reflectivity data). The periodic PSi structure used in this work was an apodized Bragg

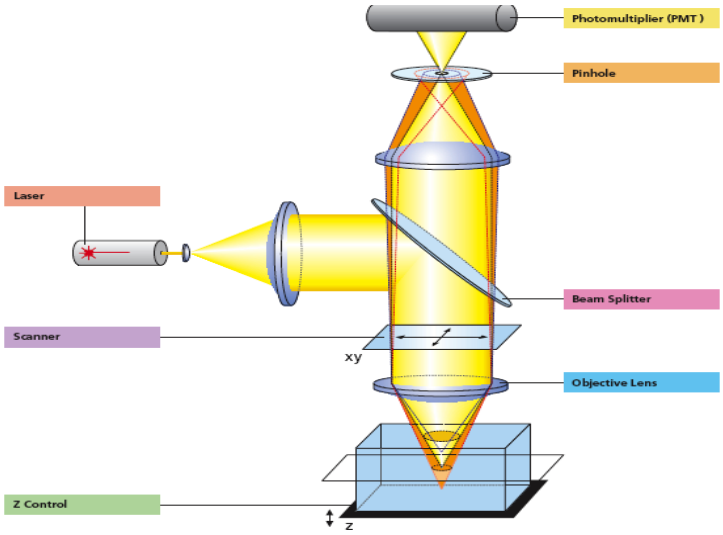

Figure 1. A schematic diagram of the confocal microscopy system (image from the Internet, modified).

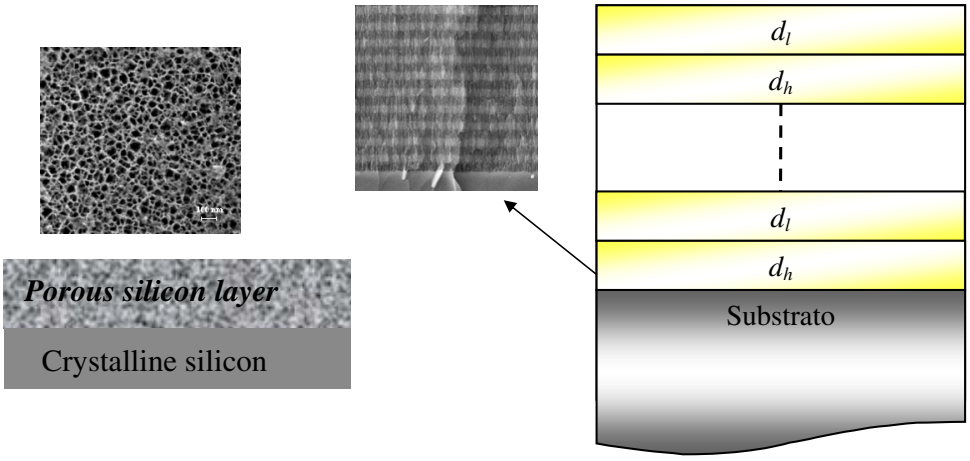

Figure 2. The porous silicon optical devices used in the experiment: a monolayer (the SEM image is a top view), and a Bragg mirror (the SEM image is a cross section). The bar scale is the same in both the SEM images.

reflector obtained by alternating high (A) refractive index layers (low porosity) and low (B) refractive index layers (high porosity) whose thicknesses satisfy the following relationship: $n_A d_A + n_B d_B = m\lambda/2$, where m is an integer and λ is the Bragg resonant wavelength. A current density of 148 mA cm^{-2} for 2.31 s was applied to obtain the low refractive index layer (effective refractive index $n_{\mathrm{L}} \cong 1.505$, thickness $d_{\mathrm{L}} \cong 598$ nm) with a porosity of 72%, while one of 110 mA cm^{-2} was applied for 2.34 s for the high index layer ($n_{\mathrm{H}} \cong 1.585$, thickness $d_{\mathrm{H}} \cong 568$ nm) with a porosity of 69%. The low contrast in the layer porosities was chosen to promote liquid infiltration of biological solutions. A schematic representation of the PSi optical structures designed and realized is reported in figure 2. The PSi microphotographs were registered by a field emission gun scanning electron microscope JEOL 6700F.

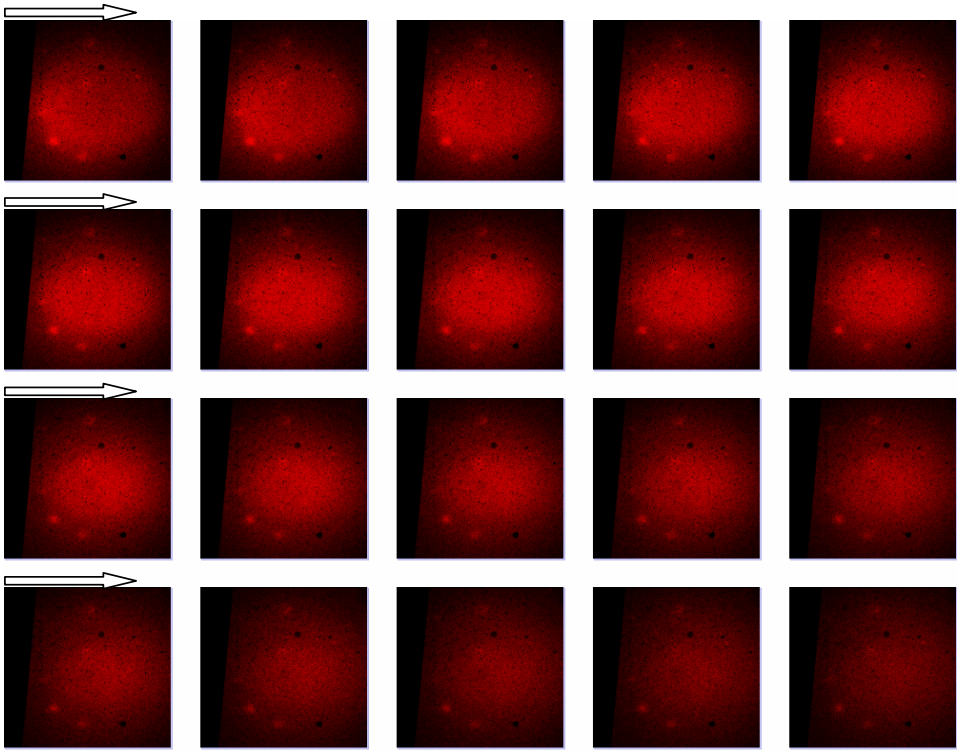

Figure 3. Sequence of confocal microscope images of the protein infiltrated monolayer. The first image is the porous silicon surface, the last is the bottom of the structure, and the arrows indicate the succession.

The PSi surface was chemically modified to covalently link a protein through its amino residues. The procedure has been described in detail elsewhere [14]. The labelled protein used to image the PSi inner distribution is the D-trehalose/D-maltose-binding protein (TMBP) is one component of the trehalose (Tre) and maltose (Mal) uptake system which, in the hyperthermophilic *archaeon T. litoralis*, is mediated by a protein-dependent ATP-binding cassette (ABC) system transporter [15]. TMBP from *T. litoralis* is a monomeric 48 kDa two-domain macromolecule containing 12 tryptophan residues [16]. Details of purification, preparation, and labelling of TMBP can be found in the literature [17]. We placed a drop on the PSi chip 20 μl of 7.5 μM sodium bicarbonate buffer (pH 7.35) containing a rhodamine-labelled TMBP and incubated the system at $-4\,^{\circ}$C overnight. We chose this kind of protein since bioprobes coming from extremophiles organisms are very stable with no loss of activity at room temperature.

3. Experimental results

Figures 3 and 4 show the sequence of confocal laser scanning microscope images (200 μm $\times$ 200 μm scan size) of the PSi monolayer and the PSi Bragg multilayer, both infiltrated by the rhodamine-labelled TMBP, respectively. All images were obtained using the 488 nm Ar laser line: at this wavelength, the penetration depth of the radiation is very short, so the fluorescent signal originates from the confocal plane in the sample. The first image is the one of the top surface and the last is the one recorded at the bottom: it is very evident that the maximum

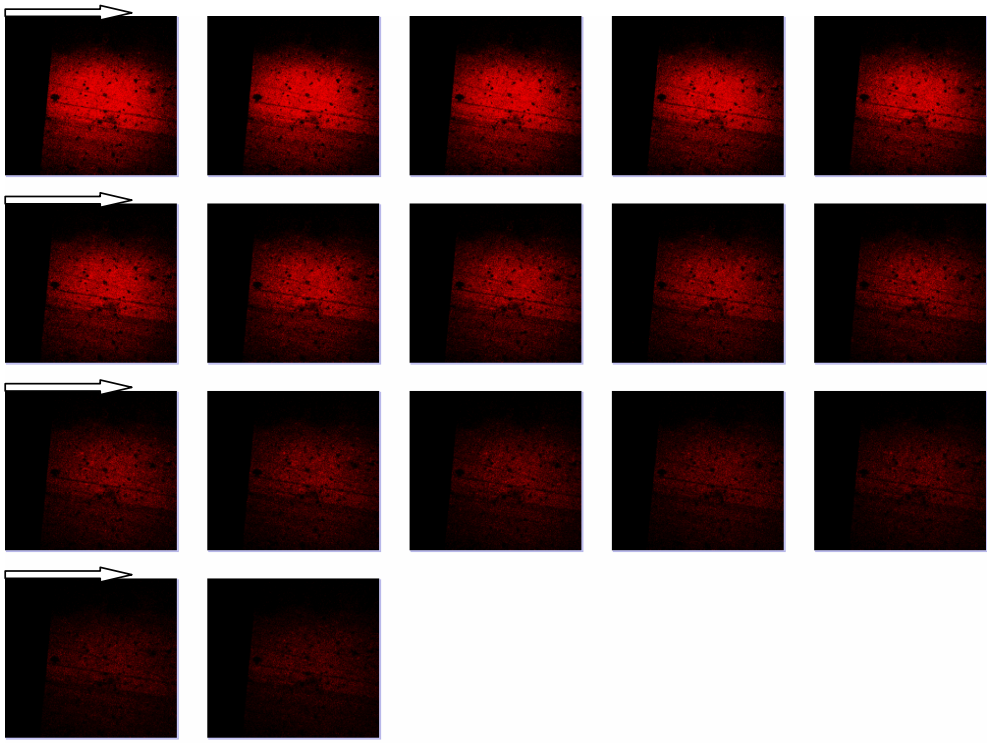

Figure 4. Sequence of confocal microscope images of the protein infiltrated Bragg multilayer. The first image is the porous silicon surface, the last is the bottom of the structure, and the arrows indicate the succession.

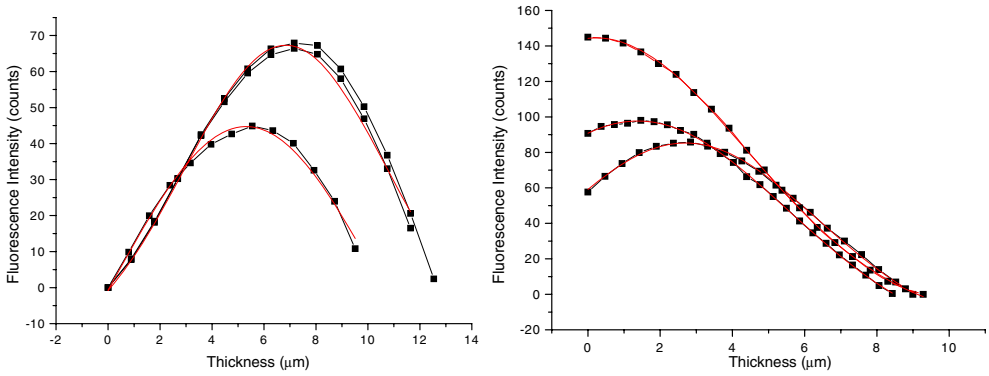

Figure 5. Intensity profiles of the fluorescence estimated by averaging the intensities of different images (three to five) concerning the same sample. Left graph: fluorescence profiles in two different porous silicon monolayers. Right graph: fluorescence profiles in the porous silicon Bragg mirror.

intensity obtained is not on top of the surface. Moreover, the fluorescent intensity is not constant along the z scanning direction. To overcome the qualitative nature of these results, we averaged the fluorescent intensities of several z-lines (three to five) through the whole PSi bulk volume. In figure 5, we report the intensity profiles of the average fluorescence signal in the case of two

different zones of the porous silicon monolayer (left graph) and Bragg mirror (right graph). The intensity values reported have been normalized to the zero signal, which is the signal obtained at the bottom of each structure. These semi-quantitative results for the two optical devices are strikingly different: in the case of the PSi monolayer, i.e. a layer having a fixed porosity, the labelled proteins are distributed as a Gaussian function having its maximum value near at the centre of the layer; the experimental data are fitted by a Gaussian curve with an $R^2 = 0.997$. Also in the case of the Bragg sequence the data are well fitted by a Gaussian law ($R^2 = 0.996$), but the maximum value is always found near the top surface. The Gaussian behaviour of the protein distribution is somewhat expected since it conforms to the solution of the diffusion equation of liquids in porous media above the percolation threshold, which is the case of the PSi considered here [18]. The thicknesses estimated from the intensity profiles are in a good agreement with the designed ones. The differences can be easily understood in terms of the geometries of the two PSi structures: the alternation of high and low porosity layers prevents a homogeneous distribution of the bioprobes which are liquid infiltrated into the spongy volume.

4. Conclusions

In this work, confocal laser scanning microscopy has been used to image the distribution of labelled protein inside the porous matrix of different PSi optical structures. There is a noteworthy difference between samples having a fixed porosity and others constituted by alternating layers of low and high porosity. In particular, we believe that this periodic sequence of PSi layer prevents a symmetric distribution of the biomolecules into the bulk volume of the porous silicon. Even if only semi-quantitative, the results obtained here are a useful indication in the design and realization of PSi-based optical affinity biosensors for genomic and proteomic applications.

Acknowledgments

We would like to thank Mr Salvatore Arbucci for his kindness in making the confocal microscopy measurements and Drs L Rotiroti and A Vitale for protein purification and sample preparation.

References

[1] Canham L 1997 *Properties of Porous Silicon* (London: INSPEC)
[2] Lin V S-Y, Motesharei K, Dancil K-P S, Sailor M J and Ghadiri M R 1997 *Science* **278** 840
[3] De Stefano L, Rotiroti L, Rea I, Rendina I, Moretti L, Di Francia G, Massera E, Arcari P, Lamberti A and Sangez C 2006 *J. Opt. A: Pure Appl. Opt.* **8** S540–4
[4] Snow P A, Squire E K, Russel P St J and Canham L T 1999 *J. Appl. Phys.* **86** 1781–4
[5] De Stefano L, Rea I, Rendina I, Rotiroti L, Rossi M and D'Auria S 2006 *Phys. Status Solidi* a **203** 886–91
[6] Pacholski C, Sartor M, Sailor M J, Cunin F and Miskelly G M 2005 *J. Am. Chem. Soc.* **127** 11636–45
[7] DeLouise L A and Miller B L 2004 *Mater. Res. Soc. Symp. Proc.* **782** A5.3.1
[8] Chan S, Li Y, Rothberg L J, Miller B L and Fauchet P M 2001 *Mater. Sci. Eng.* C **15** 277–82
[9] Ouyang H, Striemer C and Fauchet P M 2006 *Appl. Phys.* **88** 163108
[10] Paddock S W (ed) 1999 *Confocal Microscopy: Methods and Protocols* (Totowa, NJ: Humana Press)
[11] Ribes A C, Damaskinos S, Dixon A E, Carver G E, Peng C, Fauchet P M, Sham T K and Coulthard I 1995 *Appl. Phys. Lett.* **66** 2321
[12] Ribes A C, Damaskinos S, Dixon A E, Ellis K A, Duttagupta S P and Fauchet P M 1995 *Prog. Surf. Sci.* **50** 295
[13] De Stefano L, Vitale A, Rea I, Staiano M, Rotiroti L, Labella T, Rendina I, Aurilia V, Rossi M and D'Auria S 2007 Enzymes and proteins from extremophiles as hyperstable probes in nanotechnology: the use of D-trehalose/D-

maltose-binding protein from the hyperthermophilic archaeon *Thermococcus litoralis* for sugars monitoring *Extremophiles* at press
[14] Xavier K B, Martins L O, Peist R, Kossmann M, Boos W and Santos H 1996 High-affinity maltose/trehalose transport system in the hyperthermophilic archaeon *Thermococcus litoralis J. Bacteriol.* **178** 4773–7
[15] Diez J, Diederichs K, Greller G, Horlacher R, Boos W and Welte W 2001 The crystal structure of a liganded trehalose/maltose-binding protein from the hyperthermophilic archaeon *Thermococcus litoralis* at 1.85 A *J. Mol. Biol.* **305** 905–15
[16] de Champdorè M, Staiano M, Aurilia V, Stephanenko O V, Parracino A, Rossi M and D'Auria S 2006 *Rev. Environ. Sci. Biotech.* **5** 233–42
[17] De Stefano L, Rossi M, Staiano M, Mamone G, Parracino A, Rotiroti L, Rendina I, Rossi M and D'Auria S 2006 *J. Proteome Res.* **5** 1241–5
[18] Varadhan S R S 1980 *Diffusion Problems and Partial Differential Equations* (Berlin: Springer)